Title

Loss of myogenic potential and fusion capacity of muscle stem cells isolated from contractured muscle in children with cerebral palsy

Journal

American Journal of Physiology - Cell Physiology, 315(2)

ISSN

0363-6143

Authors

Domenighetti, Andrea A
Mathewson, Margie A
Pichika, Rajeswari
et al.

Publication Date

2018-08-01

DOI

10.1152/ajpcell.00351.2017

Peer reviewed

Am J Physiol Cell Physiol 315: C247–C257, 2018.
First published April 25, 2018; doi:10.1152/ajpcell.00351.2017.

RESEARCH ARTICLE

Loss of myogenic potential and fusion capacity of muscle stem cells isolated from contractured muscle in children with cerebral palsy

Andrea A. Domenighetti,[1,2,3] Margie A. Mathewson,[4] Rajeswari Pichika,[1] Lydia A. Sibley,[1] Leyna Zhao,[5] Henry G. Chambers,[6] and Richard L. Lieber[1,2,3]

[1]*The Shirley Ryan AbilityLab, Chicago, Illinois;* [2]*Department of Physical Medicine & Rehabilitation, Northwestern University, Chicago, Illinois;* [3]*Department of Orthopaedic Surgery, University of California, San Diego, La Jolla, California;* [4]*Bioengineering Department, University of California, San Diego, La Jolla, California;* [5]*ACEA Biosciences Incorporated, San Diego, California; and* [6]*Children's Hospital and Health Center, San Diego, California*

Submitted 2 January 2018; accepted in final form 18 April 2018

Domenighetti AA, Mathewson MA, Pichika R, Sibley LA, Zhao L, Chambers HG, Lieber RL. Loss of myogenic potential and fusion capacity of muscle stem cells isolated from contractured muscle in children with cerebral palsy. *Am J Physiol Cell Physiol* 315: C247–C257, 2018. First published April 25, 2018; doi:10.1152/ajpcell.00351.2017.—Cerebral palsy (CP) is the most common cause of pediatric neurodevelopmental and physical disability in the United States. It is defined as a group of motor disorders caused by a nonprogressive perinatal insult to the brain. Although the brain lesion is nonprogressive, there is a progressive, lifelong impact on skeletal muscles, which are shorter, spastic, and may develop debilitating contractures. Satellite cells are resident muscle stem cells that are indispensable for postnatal growth and regeneration of skeletal muscles. Here we measured the myogenic potential of satellite cells isolated from contractured muscles in children with CP. When compared with typically developing (TD) children, satellite cell-derived myoblasts from CP differentiated more slowly (slope: 0.013 (SD 0.013) CP vs. 0.091 (SD 0.024) TD over 24 h, $P < 0.001$) and fused less (fusion index: 21.3 (SD 8.6) CP vs. 81.3 (SD 7.7) TD after 48 h, $P < 0.001$) after exposure to low-serum conditions that stimulated myotube formation. This impairment was associated with downregulation of several markers important for myoblast fusion and myotube formation, including DNA methylation-dependent inhibition of promyogenic integrin-β 1D (ITGB1D) protein expression levels (−50% at 42 h), and ~25% loss of integrin-mediated focal adhesion kinase phosphorylation. The cytidine analog 5-Azacytidine (5-AZA), a demethylating agent, restored ITGB1D levels and promoted myogenesis in CP cultures. Our data demonstrate that muscle contractures in CP are associated with loss of satellite cell myogenic potential that is dependent on DNA methylation patterns affecting expression of genetic programs associated with muscle stem cell differentiation and muscle fiber formation.

cerebral palsy; contracture; integrins; myoblast; satellite cell

INTRODUCTION

Cerebral palsy (CP) is a neurologically nonprogressive condition caused by a perinatal insult to the brain (22, 40). Although the brain lesion is nonprogressive, children with CP have dramatic and progressive changes to their skeletal muscles including altered muscle transcriptional profile, change in connective tissue composition, and reduced force-generating capacity secondary to both central and peripheral factors (5, 51–53). CP is also associated with development of spasticity (i.e., abnormal increase in muscle tone or stiffness), shorter muscles, abnormal bony torsions, gait deviations, and development of debilitating muscle contractures, which manifest as a reduced range of joint excursion (4, 10, 21, 35). Given the stable and high prevalence of 2–3 per 1,000 births, CP places a significant and long-lasting burden on patients, families, and society (6, 11, 57). Restoring muscle strength and function, while managing spasticity and progression of muscle contracture, is the fundamental goal of rehabilitation and surgery in children with CP. Conservative treatments include physical and occupational therapies, as well as spasticity management using focal or systemic drugs and surgical intervention to release tendons, lengthen muscles, or correct bony deformities (10, 16, 20, 24, 41). Despite the variety of potential interventions among children with CP, one in three cannot walk, and among those who can walk, one in six regularly use walking aids and may lose the capacity to walk during adolescence (40). Therefore, there is an urgent need for new innovative therapeutic approaches to improving rehabilitation outcomes and the quality of life in this patient population. Currently, the biological causes for skeletal muscle impairment and development of contractures in children with CP are largely unknown, and there is much to be gained from understanding fundamental skeletal muscle adaptations at the cellular level.

Satellite cells (SCs), the muscle resident stem cells that anatomically reside in their niche between the muscle fiber and its basal lamina, are indispensable for postnatal muscle growth and regeneration (17, 30, 31, 45). Cultured mononucleated SCs, and their differentiation into fusion-competent myoblasts and then into multinucleated myotubes, provide an excellent in vitro model to study many of the complex changes that occur during postnatal muscle tissue development and regeneration. Our recently published work demonstrated a 60%–70% decrease of resident SC number in contractured muscle tissue in children with CP (14, 50). Furthermore, we recently used Pax7-DTA (Pax7CreER/+;Rosa26DTA/+) mice to reduce the muscle resident SC number to the same extent as observed in children with CP (28). Experiments on these mice showed that stretch- and casting-induced sarcomere adaptation, muscle fiber lengthening, ankle range of motion, and connective tissue

Address for reprint requests and other correspondence: A. A. Domenighetti, The Shirley Ryan AbilityLab, 26th Fl., Biologics Laboratory, 355 E. Erie St., Chicago, IL 60611 (e-mail: adomenighe@sralab.org).

homeostasis were all impaired after reduction of their SC pool. This recapitulates some of the muscle phenotype observed in young patients with CP and thus these data suggest that SC pool depletion and decreased myogenic potential of SCs could actually cause many of the muscles abnormalities in children with CP. The purpose of this study was to measure the in vitro myogenic potential of myoblasts derived from SCs isolated from children with CP and to compare it to typically developing (TD) children (Table 1). Our results suggest that SCs isolated from contractured muscles in CP have a decreased capacity to fuse and to produce myotubes in vitro. This impairment was associated with downregulation of the muscle-specific integrin-signaling pathway that regulates myoblast fusion during myotube formation. Interestingly, decreased expression of the integrin-β 1D (ITGB1D) isoform was linked to DNA hypermethylation of the CpG island located in the promoter region of the ITGB1 gene. Furthermore, the cytidine analog 5-azacytidine (5-AZA) induced demethylation of the same promoter region and thus rescued ITGB1D expression and improved myotube formation in CP cell cultures.

METHODS

Muscle biopsy collection. This study met the ethical standard of the Declaration of Helsinki and was approved by the institutional review board of the University of California, San Diego, Human Research Protection Program. Participants were recruited into this study after age-appropriate assent from children and written informed consent from parents were obtained. CP children with diplegia or quadriplegia underwent hamstring lengthening surgery involving the gracilis and semitendinosus muscles whereas typically developing (TD) children were recruited as a comparison group because they were undergoing anterior cruciate ligament (ACL) reconstructive surgery but with no previous history of neurological disorders. Children undergoing ACL replacement have recovered from the initial injury without knee swelling and demonstrate normal gait. Thus, for the purposes of this study, they are considered normal controls, which is critical because actual normal children's muscle is nearly impossible to obtain. The autograft in TD children was made using gracilis and semitendinosus tendons, which were excised along with a portion of distal muscle that was obtained as it was trimmed from the tendon. Biopsies from children with CP and TD children were obtained from the distal muscle portion near the musculotendinous junction. Exclusion criteria for CP patients included: *1*) previous traumatic leg injury such as fractures, dislocations, or ligament tears; *2*) surgery or drug treatment (e.g., Botulinum toxin, Baclofen) to the leg within the past 6 mo; and *3*) dystonia, athetosis, or other involuntary movements. Inclusion criteria included: *1*) 3–18 yr of age, *2*) diagnosis of cerebral palsy, and *3*) Gross Motor Function Classification System (GMFCS) Levels I–V. All patients with CP had developed a contracture requiring surgery, despite receiving conservative treatment. Patients were classified based on clinical measures of the GMFCS scale and popliteal angle. The GMFCS provides a description of a child's current self-initiated motor function (lower level being associated with better motor function) and gives an idea of the types of mobility aids a child may need in the future, e.g., crutches, walking frames, or wheelchairs (23). Popliteal angle is an assessment of hamstring muscle tone. The thigh is flexed on the abdomen with one hand, and then the other hand straightens the leg by pushing on the back of the ankle until there is firm resistance to the movement. There is no definition of GMFCS or popliteal angle for TD patients. On average, patients with CP were ~6 yr younger than the TD control children (yr old: 9 (SD 4) CP vs. 15 (SD 1) TD, $P < 0.005$, $n = 8$/group; Table 1). TD children were recruited as a comparison group because they were undergoing ACL reconstructive surgery using a hamstring autograft and had no history of neurological disorders. Surgery for TD patients took place ~4 mo after the initial injury of their ACL. At this time, they had no swelling, walked freely, and continued all activities of daily living, with the exception of participating in intensive sports or exercise. We believe that this level of activity for several weeks before surgery suited the TD patients to be "controls" in our study.

Table 1. *Characteristics of study participants*

Patient	Age	Sex	GMFCS	Pop Angle	Limbs	Prev Surg	BTX	Baclofen
CP1	9	M	5	110	Q	No	No	Yes
CP2	7	M	2	100	D	No	Yes	No
CP3	8	M	2	100	D	No	Yes	No
CP4	3	M	4	110	Q	No	Yes	Yes
CP5	18	F	5	100	Q	Yes	No	Yes
CP6	8	F	3	110	D	No	Yes	Yes
CP7	10	M	4	135	Q	Yes	Yes	Yes
CP8	8	F	3	120	D	No	Yes	No
TD1	16	M	NA	NA	NA	No	No	No
TD2	15	M	NA	NA	NA	No	No	No
TD3	15	M	NA	NA	NA	No	No	No
TD4	14	F	NA	NA	NA	No	No	No
TD5	16	F	NA	NA	NA	No	No	No
TD6	15	M	NA	NA	NA	No	No	No
TD7	14	F	NA	NA	NA	No	No	No
TD8	18	F	NA	NA	NA	No	No	No

Baclofen, whether patient had exposure to baclofen (>6 mo prior); BTX, whether patient had exposure to botulinum toxin (>6 mo prior); CP, cerebral palsy; D, diplegia; F, female; GMFCS, Gross Motor Function Classification System; M, male; NA, nonapplicable; Pop, popliteal; Prev surg, whether the patient had previous surgeries (>6 mo prior); Q, quadriplegia; TD, typically developing. Age measured in years; popliteal angle measured in degrees.

SC isolation. SCs were isolated by fluorescence-activated cell sorting (FACS) using a modification of the previously described procedure (50). Briefly, gracilis or semitendinosus muscle biopsies from TD and CP patients were digested in a collagenase-dispase solution, mechanically disrupted with forceps, filtered twice, spun at 600 *g* for 10 min, and resuspended in FACS buffer (pH 7.4 1 mM EDTA and 2.5% normal goat serum in PBS). Cells were stained with anti-CD56 (neural cell adhesion molecule, clone HCD56), which has previously been shown to reliably identify myogenic Pax7 + SCs (7, 50), anti-CD31 (clone EP3095), which is a marker of endothelial cells, and anti-CD45 (ab-10559, Abcam), which is a marker of leukocytes. CD31 and CD45 were combined into a dump channel and the remaining $CD56^+$ cells were collected using a FACSAria II (BD Biosciences, San Jose, CA). In this study, SCs were defined as the population of cells that were $CD31^-/CD45^-/CD56^+$. Gating was set to high stringency, including only $CD56^+$ cells and excluding double positive cells. It is possible that many SCs were discarded, but the population collected was very pure and appeared homogeneous and highly myogenic in culture. SC-derived myoblasts in culture (passages P2–P4) were used for all experiments listed below.

Fusion and differentiation assays. Myoblast fusion and myotube formation were examined in vitro using the iCELLigence RTCA Instrument (ACEA Biosciences), which measures the electric impedance of cells during growth without labeling. Electric impedance measurement assays were previously used successfully to monitor growth and formation of myotubes in vitro (39, 48). In our assays, SC-derived myoblasts were grown in modified 0.5% gelatin-coated 8-well plates with microelectrodes on the bottom of each well for impedance-based detection. Myoblasts (20,000) were seeded per well (surface area 0.64 cm^2), covering 60%–70% of well surface after settling for 12 h. Cells were cultured at 37°C in a 5% CO_2 atmosphere using a high-serum medium containing Ham's F10 (Corning) with 20% fetal bovine serum (from GIBCO), 10 mg/ml streptomycin, and 100 U/ml penicillin (GIBCO) and human recombinant bFGF (5 ng/ml,

BD Biosciences) until they were ~90% confluent. Differentiation was promoted by switching from high-serum to a low-serum DMEM medium (GIBCO) containing 2% horse serum (GIBCO), 4.5 g/l D-Glucose, L-Glutamine, 10 mg/ml streptomycin, 100 U/ml penicillin (GIBCO), and 1 μl/ml insulin solution (Sigma-Aldrich). Myotube formation was associated with a significant increase in cell impedance, measured as a baseline Cell Index (CI) increasing over time. For myotube formation quantification, CI was monitored every 15 min for up to 42 h after the switch to low-serum medium. Two to three replicates of each culture were run at the same time and averaged. Data were analyzed using the RTCA software from ACEA. After normalization and measurement of a Delta Cell Index (DCI), the slope of the curve generated, starting from the time of medium switch to the time when the assay was stopped, was used to quantify "rates of fusion and myotube formation" over time in CP versus TD samples (Fig. 1, *A* and *B*). To validate this assay, myoblast fusion index measurements and immunohistochemistry (see below) were performed in parallel.

Immunostaining. Cells were cultured in 35-mm, low 60 μ-Dish plates (Ibidi). Cultures were rinsed one time with PBS, fixed for 10 min with 4% paraformaldehyde, and rinsed three times with PBS. Cells were then permeabilized for 10 min in 1×PBS supplemented with 0.2% Triton X-100 (Sigma-Aldrich), washed three times with PBS, and incubated in blocking solution (150 mM NaCl and 20 mM Tris, pH 7.4) supplemented with 1% BSA for 1 h at room temperature before incubation with primary antibodies against slow myosin heavy chain (MYH7) (clone NOQ7.5.4D), β-tubulin (clone E7), or pan-vinculin (which detects both vinculin and metavinculin forms; clone hVIN-1) diluted in blocking solution. Cells were incubated with primary antibodies overnight at 4°C. After incubation, cells were washed three times for 5 min with PBS and incubated with secondary antibodies (all from Jackson ImmunoResearch) diluted into blocking solution for 1–2 h at room temperature. Secondary antibody mixtures also contained 4′,6′-diamidino-2-phenylindole (DAPI) and Alexa Fluor 488 conjugate of wheat germ agglutinin (WGA, Thermo Fisher Scientific) when appropriate. After washing three times with PBS for 5 min, cells were mounted using fluorescent mounting medium (Vectashield). Microscopy was performed using a Leica TCS SP5 confocal microscope using the ×20 air objective and zoom rates between one and three in sequential scanning mode when appropriate.

Fusion index. The fusion index was calculated 42 h after switch to low-serum medium. It was defined as the total number of DAPI-stained nuclei (excluding mono- and binucleated) in slow myosin heavy chain (MYH7)-positive cells cells divided by the total number of nuclei per field. The number of nuclei per myotube was established by automated count of nuclei within every myotube per microscopic field divided by the number of myotubes in the field, where a myotube is defined as a MYH7-positive cell with at least three nuclei. For each sample, the fusion index was measured using 5 microscopic fields/35-mm cell culture dish, acquired on a Leica TCS SP5 confocal microscope using the 20 × air objective.

5-AZA treatment of cultured myoblasts. Myoblasts were seeded at ~13,000 cells/cm^2 and were maintained in the same high-serum medium up to 70%–80% of confluence. These proliferating cells were then treated with 5-AZA (5 μM, Sigma-Aldrich) for 24 h to induce DNA demethylation before differentiation or not treated with 5-AZA as a control. Differentiation was promoted by switching from high-serum to the low-serum DMEM medium (GIBCO). Myotube formation was monitored and fusion indices were quantified 42 h after differentiation on fixed and immunostained cell cultures. The 5-AZA concentration of 5 μM was selected as it was previously reported as the optimal concentration to induce effects on differentiation without cytotoxicity (27, 38, 55).

Western blotting. Proteins were extracted from cells by briefly sonicating samples suspended in custom-made RIPA buffer (1.752 g NaCl, 2 ml NP-40, 1 g deoxycholic acid, 1 ml 20% SDS, 6.67 ml 1.5 M Tris, pH 8, to 200 ml with ddH_2O), followed by 4°C centrifugation (10,000 *g*, table-top centrifuge with FA-45-24-11 rotor, Eppendorf) to remove membrane components. Protein samples were stored in custom-made radioimmunoprecipitation assay buffer at −80°C. Total proteins (15 μg) were separated using NuPAGE 4%–12% Bis-Tris gels with 20 × NuPAGE MES or MOPS SDS running buffers and antioxidants, according to manufacturer's protocols (Novex-Life Technologies). After separation, proteins were transferred to a nitro-

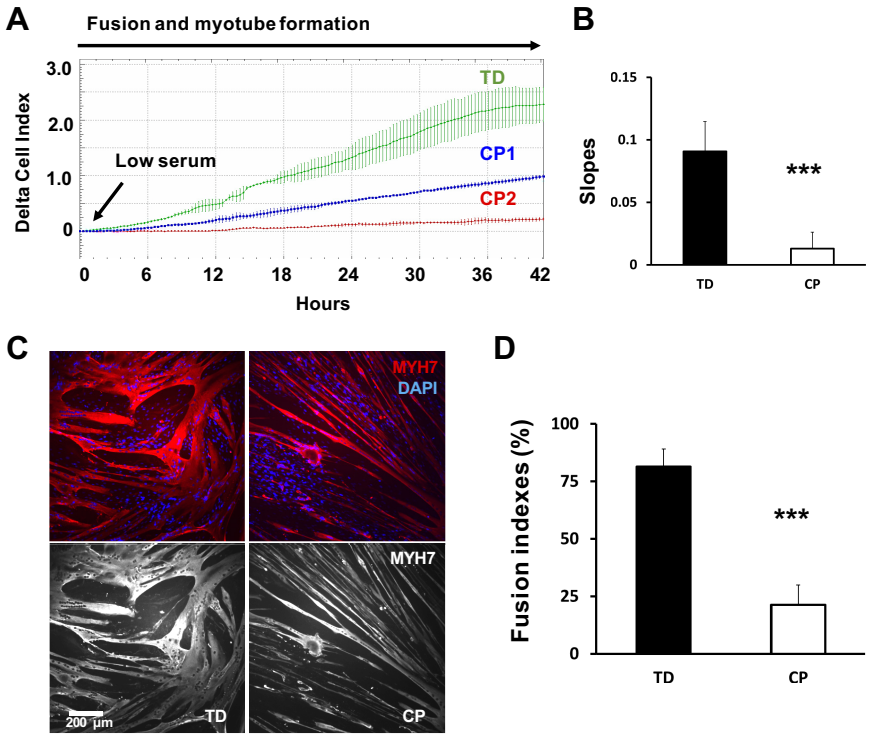

Fig. 1. Decreased myoblast fusion and myotube formation in cerebral palsy (CP). *A*: example of a normalized differentiation assay performed over ~42 h with the iCELLigence RTCA system. Green curve represents a typically developing (TD) myoblast preparation (average of 3 wells). Blue and red curves correspond to cell preparations from two different CP children, CP1 and CP2, under the same conditions (average of 3 wells per sample). Differentiation was promoted by switching from high-serum to low-serum medium. Myotube formation is associated with a significant increase in cell impedance. *B*: slopes of growth curves are used to quantify the rate of fusion and myotube formation over time; ***CP vs. TD, $P < 0.001$; analysis by one-way ANOVA ($n = 8$/group). *C*: myoblasts from CP and TD preparations were differentiated for 42 h and stained for slow myosin heavy chain (MYH7) and a nuclear stain (4′,6′-diamidino-2-phenylindole, DAPI). CP myotubes appeared spindly, thin, and with fewer nuclei per myotube. Gray scale panels show MYH7 staining as a single channel. *D*: quantification of fusion index for CP and TD myoblasts. Quantification was performed after 42 h of differentiation; ***CP vs. TD, $P < 0.001$; Analysis by one-way ANOVA ($n = 8$/group).

cellulose membrane in a Tris-glycine buffer complemented with 20% methanol. To visualize bands and detect transfer efficiency, membranes were stained with Ponceau S membranes were then blocked in a buffer containing 10 mM Tris, 0.15 M NaCl, 0.1% Tween-20, and 1% BSA and incubated with the primary antibody (1:500 to 1:1,000 dilution) overnight at 4°C. After washing, membranes were incubated with peroxidase-conjugated secondary antibodies (1:1,000 dilution) for 1 h at room temperature (all from Jackson ImmunoResearch) and bands identified using chemiluminescence (ECL). Bands were analyzed by densitometry on a PXi imager (Syngene), and values are expressed as arbitrary values of protein levels, normalized by total proteins transferred on nitrocellulose membrane (as visualized with Ponceau S). Primary antibodies used were: MYH7 (clone NOQ7.5.4D), pan-vinculin (clone hVIN-1), SR Ca^{2+}-ATPase (SERCA1; clone VE121G9), ITGB1D (custom-made, a kind gift from Dr. Robert S. Ross, M.D., University of California, San Diego), total and phosphorylated focal adhesion kinase (FAK; FAK antibodies Sampler Kit no. 9330, Cell Signaling Technology).

Real-time PCR. Myoblasts, pretreated or nontreated with 5 μM 5-AZA for 24 h, were cultured in high serum medium until they reached 80–90% confluence. After switch to low-serum medium, myoblast preparations were allowed to differentiate for 24–72 h before RNA extraction. Total RNA was isolated and purified from myoblast cell culture preparations using Trizol reagent (Ambion, Life Technologies) according to the manufacturer's recommendations. First-strand cDNA synthesis from purified RNAs and qPCR amplification was performed using the GoTaq 2-Step RT-qPCR System kit (Promega) according to manufacturer's protocols. Resulting cDNAs were subjected to SYBR Green-based real-time amplification using a C1000 Thermal Cycler apparatus (Bio-Rad). Each PCR amplification reaction (20-μl volume) contained 100 ng of starting cDNA template. Gene expression profiling during myoblast differentiation was investigated using predesigned 96-well gene panels for use with SYBR Green (SABioscience) (Supplemental Material Tables S1 and S2; Supplemental Material for this article is available online at the Journal website). The panels utilized expertly designed and experimentally validated PCR primers and assays and included three reference genes for relative gene expression normalization and quantification: HPRT1, TBP, and AP3DI. These reference genes were specifically validated for our experimental treatment and conditions and were selected among 15 experimentally tested candidates and analyzed using the software packages Bestkeeper, geNorm, and Normfinder (15, 25). Cycling conditions for SYBR Green primers consisted of an initial step at 50°C (2 min) and a first denaturizing step at 95°C (2 min), followed by 50 cycles of a thermal step protocol consisting of 95°C (20 s), 60°C (20 s), and 72°C (20 s). A standard melt curve profiling consisting of a 65°C–95°C thermal ramp was performed at the end of each protocol. Gene expression quantification was performed using Bio-Rad CFX Manager software. Positively and negatively regulated genes were selected following a $P < 0.05$ and a 2 or 0.5 expression level, respectively. Functional gene classification was performed using the Database for Annotation, Visualization and Integrated Discovery (DAVID; version 6.8; https://david.ncifcrf.gov/).

ITGB1 promoter methylation analysis. The promoter region of the human *ITGB1* gene contains CpG islands at position 32957344-32958779 on chromosome 10 (band: 10p11.22; genomic size: 1436; UCSC Genome Browser on Human Dec. 2013 GRCh38/hg38 assembly). To test for ITGB1 promoter methylation, we used a Promoter Methylation PCR Kit (Affymetrix). In this experiment, isolated genomic DNA was digested with MseI restriction enzyme, and the resulting DNA fragments were incubated with the DNA methylation binding protein MeCP2/MBP. Methylated DNA fragments were isolated with a spin column and then amplified with promoter specific primers encompassing CpG sites. Real-time qPCR was used to amplify PCR products using similar cycling conditions reported above. The presence of an amplified product indicated that a specific promoter region was methylated in the genomic DNA sample. Two primer pairs targeting different regions of the CpG island in the ITGB1 promoter were designed: CpG 1F = CCTTCGCAGAGGAGGAAACT, CpG 1R = CTCCGGAAACGCATTCCTCT; CpG 2F = GGTAGAAGTTGGCTTAGTGG, CpG 2R = ACGCGGTAAAATGATACTAGAC. These primers encompassed DNA regions containing 15 and 19 CpG dinucleotides, respectively. An additional primer pair encompassing a region of the promoter without CpG sites was used as a negative control: CTRL *F* = CAGTTTTCTGTGCTGAGACTGG, CTRL R = CCCACTTAATGGATGTTCAAGC.

Statistics. Results are expressed as mean values with standard deviation (SD). Analysis of variance (ANOVA), both one-way and two-way, was used to test for differences ($P < 0.05$) between CP and TD groups (i.e., "condition"), and other independent variables, such as "time course" or "treatment." When statistical significance was achieved, post hoc analysis using Tukey's *t*-test with the Bonferroni correction was applied. Linear regression quantified the correlation between iCELLigence-generated slope and fusion indices (Fig. 2).

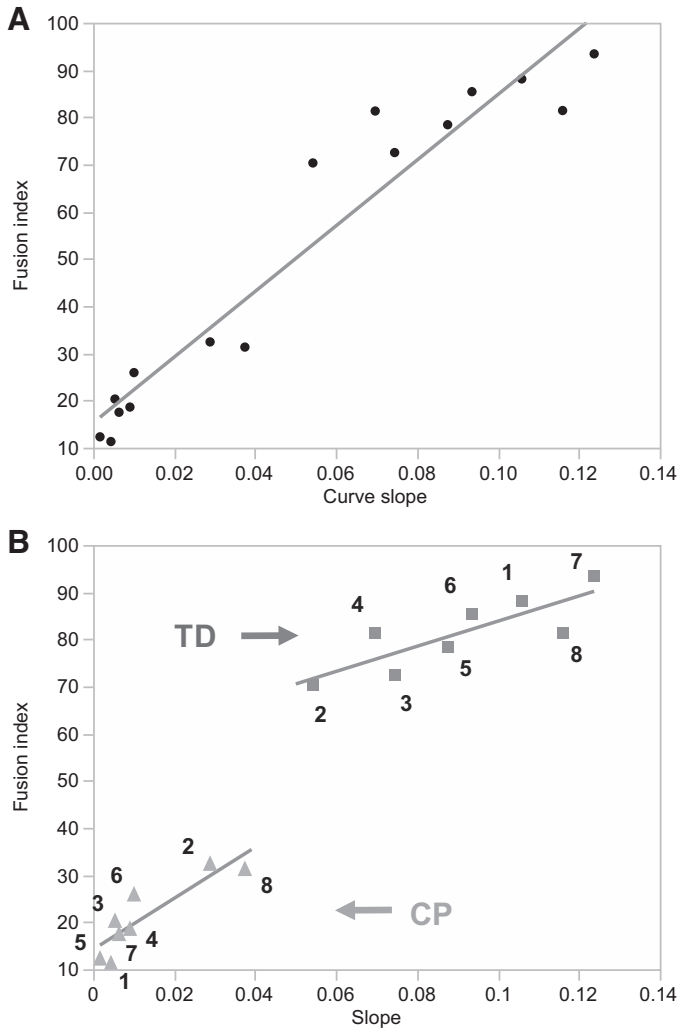

Fig. 2. Linear regression of electric impedance measurements and fusion index. A significant correlation between these values was observed. *A*: regression analysis for all the values (CP and TD combined); $R^2 = 0.92$, $P < 0.0001$. *B*: regression analysis for separated TD (squares) and CP (triangles) values; TD ($R^2 = 0.68$, $P = 0.01$), CP ($R^2 = 0.77$, $P = 0.004$). Squares (TD) and triangles (CP) are numbered from 1 to 8. These numbers correlate with patient identification numbers (e.g., number 1 next to a square = patient TD1). All three analyses showed a significant correlation between electric impedance measurements and fusion index, thus validating the impedance method. CP, cerebral palsy; TD, typically developing.

Analysis was performed using software package JMP13 Pro (SAS).

RESULTS

Impaired myoblasts fusion and myotube formation in CP cell cultures. Cell impedance measurements over a 42-h period demonstrated that rates of fusion and myotube formation were decreased by ~85% in CP cultures compared with TD (slope: 0.013 (0.013 SD) CP vs. 0.091 (0.024 SD) TD, $P < 0.001$) (Fig. 1, *A* and *B*). Analogous measures of fusion index showed that there was a ~74% decrease of fusion index in CP myoblast cultures compared with TD, 42 h after differentiation (21.3 (8.6 SD) CP vs. 81.3 (7.7 SD) TD, $P < 0.001$) (Fig. 1, *C* and *D*). Linear regression showed a highly significant correlation between electric impedance measurements and fusion index ($R^2 = 0.92$, $P < 0.001$, CP and TD values combined), validating the slope of the curves generated by impedance measurements as a valid assay to quantify fusion and myotube formation in vitro (Fig. 2).

Immunostaining of cultured myotubes was used to investigate morphological changes in CP versus TD cell cultures after 42 h of differentiation. Cultures from the two groups differed dramatically, with more mononucleated myoblasts and fewer thin, spindly myotubes forming in CP cultures compared with the many thick and highly multinucleated myotubes in TD cultures (Fig. 1*C* and Fig. 3). Western blots showed significant downregulation of important protein markers of myoblast differentiation and myotube maturation in CP cultures, including MYH7, metavinculin (MV), and the SR Ca^{2+}-ATPase SERCA1/ATP2A1 after both 4 h and 42 h of differentiation in low-serum medium (Fig. 4). Together, these data demonstrate significant changes in fusion capacity and myotube formation in CP myoblasts compared with TD. The high expression level of markers such as MYH7, MV, and SERCA1/ATP2A1 in TD cell cultures after 48 h indicated that these cells differentiated faster and matured further down the myogenic pathway compared with CP cultures.

Gene expression profiling during myoblast differentiation in CP. Real-time qPCR was used to analyze the expression of a curated panel of 85 genes that were previously shown to be involved in myogenesis and skeletal muscle remodeling. Our data showed that among 85 genes investigated, 42 were significantly downregulated, and 9 were significantly upregulated in CP cell cultures compared with TD 24 h after differentiation (Supplemental Table S1). Among the downregulated candidates were genes involved in the scaffolding and contractile system of the muscle fiber (e.g., *ACTA1*, *ACTA2*, *TNNI3*, *DES*, *TPM1*), myogenic factors (e.g., MEF2C, MEF2A, MYF5, MYF6, CDK5, PAX3), vesicle trafficking (CAV1, CAV3), mitogen-activated protein kinase (MAPK14), Wnt/β-catenin, and sonic hedgehog signaling (CTNNB1, SHH), and members of the integrin signaling pathway (ITGA7, ITGB1, ITGAV, CAV3). These data suggest that loss of myogenic potential could be driven by a global downregulation of genes and signaling pathways involved in myoblast fusion and muscle fiber maturation in CP.

Downregulation of the integrin signaling pathway during myoblast differentiation in CP. One molecule that mediates integrin receptor signaling is the protein tyrosine kinase FAK. Phosphorylation of FAK is transiently increased during myogenic differentiation, and inhibition of this process blocks myoblast fusion (42). Protein analysis showed significant suppression of ITGB1D levels (Fig. 5, *A* and *B*) and FAK phosphorylation at residues Y576–7 and Y925 in CP myoblasts after 4 and 42 h of differentiation in low-serum medium (Fig. 5, *D* and *E*). No differences were noted for total FAK or autophosphorylating FAK Y397 levels between CP and TD

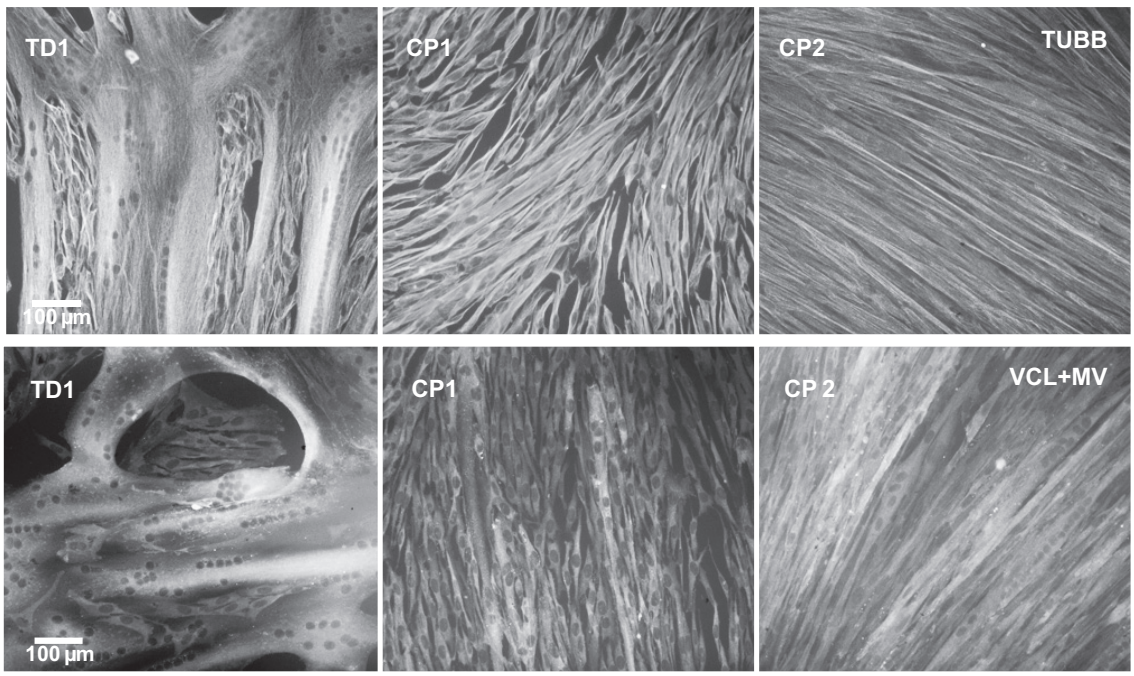

Fig. 3. Impaired fusion and myotube formation in cerebral palsy (CP) myoblast cultures. Immunofluorescence stain for the same typically developing (TD) and CP (CP1 and CP2) myotube preparations shown in Fig. 1*A*. Grayscale panels show myoblast preparations differentiated for 42 h and then immunostained for β-tubulin (TUBB) or pan-vinculin, which detects vinculin (VCL) and metavinculin (MV).

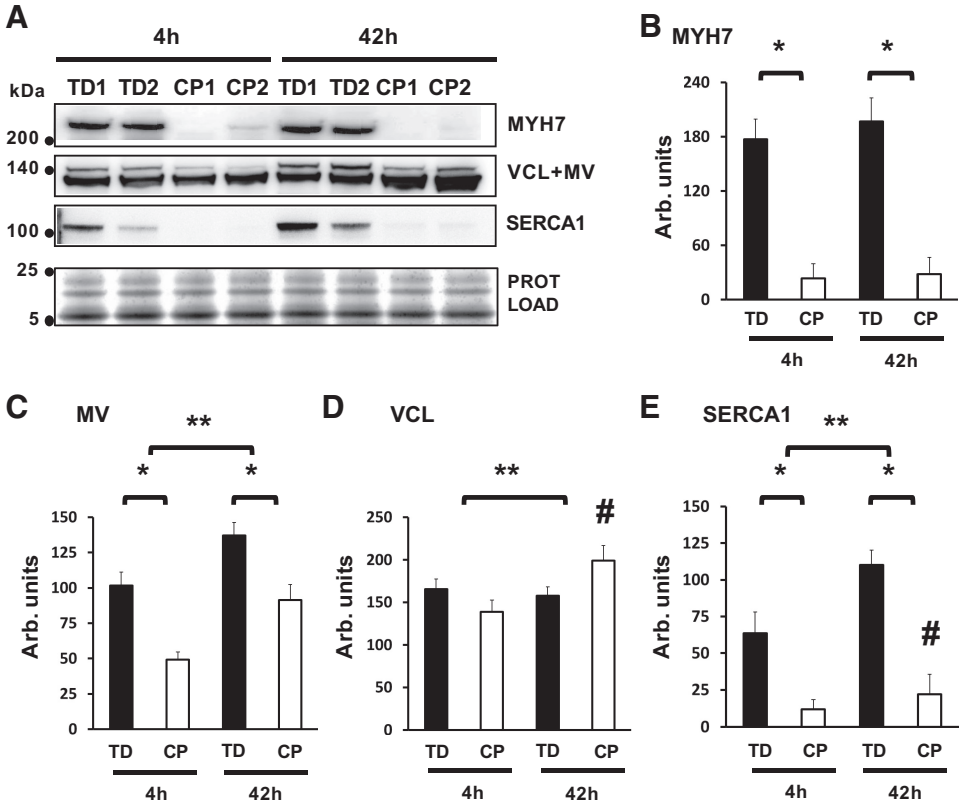

Fig. 4. Protein expression shows decreased myotube maturation in cerebral palsy (CP). *A*: representative Western blots showing differential expression of slow myosin heavy chain (MYH7, bands at ~223 kDa), vinculin (VCL, lower band, ~120 kDa), and metavinculin (MV, upper band, ~145 kDa) on the same membrane, SR Ca^{2+}-ATPase 1 (SERCA1, ~110 kDa), and total protein load (bands in the 5–25 kDa range). Protein analysis was performed in CP and typically developing (TD) cell preparations 4 h (4h) and 42 h (42h) after medium switch. *B*: protein quantification for MYH7; *CP vs. TD, $P < 0.0001$; Analysis by two-way ANOVA ($n = 6$/group). *C*: protein quantification for MV; *CP vs. TD, $P < 0.0001$, **4 h vs. 42 h, $P < 0.0001$; Analysis by two-way ANOVA ($n = 6$/group). *D*: protein quantification for VCL; **4 h vs. 42 h, $P = 0.0001$, #CP after 42 h, $P < 0.0001$, Analysis by two-way ANOVA ($n = 6$/group). *E*: protein quantification for SERCA1, *CP vs. TD, $P < 0.0001$, **4 h vs. 42 h, $P < 0.0001$, #CP after 42 h, $P = 0.0009$; Analysis by two-way ANOVA ($n = 6$/group). Only significant *P* values are reported.

preparations, even though myoblast differentiation between 4 and 42 h was associated with an increase of FAK Y397 in both CP and TD cell preparations (Fig. 5, *A* and *C*). These data demonstrate that loss of myogenic potential and gene repression in CP myoblasts was associated with impairment of integrins signaling during myotube formation in vitro.

5-AZA rescues ITGB1D expression and promotes myotube formation in CP. The ITGB1D isoform is upstream of FAK as an integrin receptor β-subunit and is also regulated at the gene level by FAK phosphorylation, which suggests that bidirectional signaling could affect the ITGB1D–FAK pathway during myoblast fusion (42). To further investigate potential mechanisms that could inhibit ITGB1D expression during myoblast fusion and myotube formation in CP, we performed a DNA methylation analysis of the promoter region of the human ITGB1 gene. DNA methylation is an epigenetic mechanism used by cells to silence gene expression in a mitotically inheritable fashion. Changes in DNA methylation of muscle-specific genes as well as in gene promoter and enhancer regions enriched for CpG dinucleotides (CpG islands) play a critical role in regulating myogenic differentiation in SCs (8, 9, 29). DNA methylation analysis of the CpG island located in the promoter region of the ITGB1 gene showed a ~sevenfold increase in promoter DNA methylation levels in CP myoblasts after 24 h of differentiation (Fig. 6*A*). A 24-h pretreatment of myoblast cultures with 5 μM of demethylating agent 5-AZA before differentiation was sufficient to demethylate the CpG island in the ITGB1 promoter region (Fig. 6*A*) and increase ITGB1D protein expression levels in differentiating CP cultures (Fig. 6, *D* and *E*). Morphologically, 24 h of 5-μM 5-AZA pretreatment of myoblast cultures was sufficient to increase the fusion index more significantly in CP myoblasts (200% increase, 16.0 (4.9 SD) CP vs. 48.1 (9.6 SD) CP-AZA after 48 h) compared with TD myoblasts (18% increase, 75.4 (6.6 SD) TD vs. 89.4 (5.8 SD) TD-AZA after 48 h) (Fig. 6, *B* and *C*).

Differential gene expression profiling after 5-AZA treatment in CP cell culture. To investigate whether additional signaling pathways and genes were affected by 5-AZA treatment, real-time qPCR was used to analyze the expression of 91 genes involved in myogenesis, neurogenesis, and adipogenesis in fusing CP myoblasts after 24 h of pretreatment with 5 μM of 5-AZA (Supplemental Table S2). We found that 43 genes were significantly upregulated and 7 genes were significantly downregulated in cultures pretreated with 5-AZA compared with nontreated CP cultures after 48–72 h of differentiation. Several candidate genes that were found to be initially downregulated in differentiating CP cultures when compared with TD (Supplemental Table S1) showed a pattern of upregulation after 5-AZA treatment in CP (*ACTA1*, *BMI1*, *CAV3*, *DES*, *FOXO1*, *ITGA7*, *ITGB1*, *MEF2A*, *MEF2C*, *MET*, *MYF5*, MYF6, *NOTCH2*, *PAK1*, *PAX3*, *PPARA*, *PPARD*, *SHH*, *SIX1*). Also, 5-AZA pretreatment led to upregulation of transcription regulators involved in myogenesis and other signaling pathways (BMI1, SIX1, SIX4, EGR3, FOXO1, MAPK14, MEF2A, MEF2C, MYF5, MYOG, NEUROD2, NOTCH2, PAX3, PAX7, PPARA, PPARD, PPARG, RPBJ, RARA). Specific signaling pathways were also upregulated, including NOTCH (DLL1, JAG1, JAG2, NOTCH2, RPBJ) and the integrin and focal adhesion pathways (BCL2, MET, ACTN2, CAV3, ITGA7, ITGB1, PAK1). Interestingly, upregulation of myogenic factors was also associated with upregulation of factors potentially involved in regulatory networks of other differen-

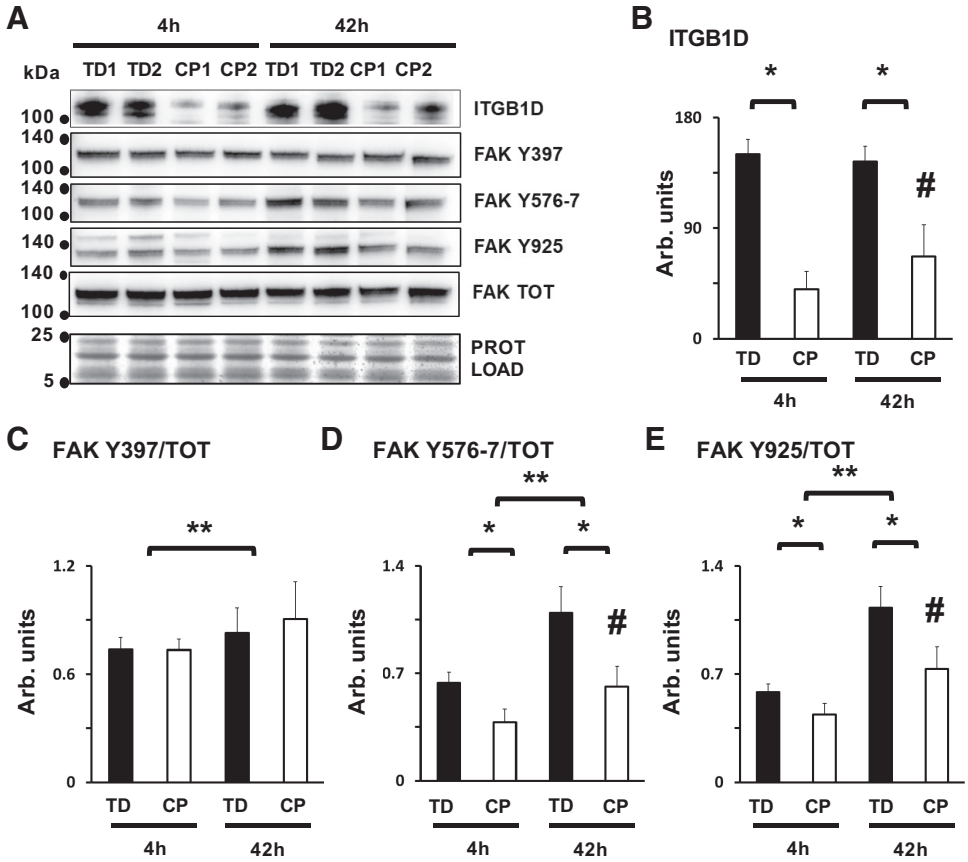

Fig. 5. Impaired integrin signaling during myoblast fusion and differentiation in cerebral palsy (CP). *A*: representative Western blots showing differential expression of integrin β-1D (ITGB1D, bands at ~116 kDa), focal adhesion kinase (FAK) phosphorylated at residue Y397 (FAK Y397, ~125 kDa), FAK phosphorylated at Y576/7 residues (FAK Y576/7, ~125 kDa), FAK phosphorylated at Y925 residue (FAK Y925, ~125 kDa), total FAK protein levels (FAK TOT, ~125 kDa), and total protein (bands in the 5–25 kDa range). Protein analysis was performed in CP and typically developing (TD) cell preparations, 4 h (4h) and 42 h (42h) after high- to low-serum medium switch. *B*: protein quantification of ITGB1D; *CP vs. TD, $P < 0.0001$; #CP after 42 h, $P = 0.01$, analysis by two-way ANOVA ($n = 8$/group). *C*: protein quantification for FAK Y397, normalized over FAK TOT; **4 h vs. 42 h, $P = 0.025$, analysis by two-way ANOVA ($n = 6$/group). *D*: protein quantification for FAK Y576/7, normalized over FAK TOT; *CP vs. TD, $P < 0.0001$, **4 h vs. 42 h, $P < 0.0001$, #CP after 42 h, $P = 0.034$, analysis by two-way ANOVA ($n = 6$/group). *E*: protein quantification for FAK Y925, normalized over FAK TOT, *CP vs. TD, $P < 0.0001$, **4 h vs. 42 h, $P < 0.0001$, #CP after 42 h, $P = 0.009$, analysis by two-way ANOVA ($n = 6$/group). Only significant *P* values are reported.

tiation programs, including neurogenesis and adipogenesis (NEUROD2, PPARG) (18, 19). Together, these data suggest that downregulation of integrin ITGB1D-FAK signaling pathway and decreased myogenic potential of differentiating myoblasts may be dependent on small or large-scale changes in DNA methylation patterns affecting gene expression and activation of promyogenic signaling pathways in these cells.

DISCUSSION

This study provides compelling evidence that myoblasts derived from SCs isolated from contractured CP muscle have a decreased capacity to fuse and to produce myotubes in vitro. This impairment is associated with downregulation of the muscle-specific integrin signaling pathway that regulates myoblast fusion during myotube formation. Decreased expression of the integrin-β 1D (ITGB1D) isoform during differentiation is linked to DNA hypermethylation of the CpG islands located in the promoter region of the ITGB1 gene. Twenty-four-hour pretreatment of CP myoblasts with the cytidine analog 5-AZA was sufficient to demethylate the same promoter region, rescuing ITGB1D expression and improving myotube formation during differentiation. Taken together, these data demonstrate that muscle contractures are associated with decreased myogenic potential of SCs in children with CP. Importantly, as demonstrated by 5-AZA treatment, this loss may be linked to changes in DNA methylation patterns affecting expression of genetic programs associated with SC differentiation and muscle fiber formation in CP.

The myoblast fusion process is a highly complex, integrated network involving coordination and crosstalk of many signaling pathways, including multiple adhesion molecules, transmembrane receptors, signaling pathways, and timely activation or inhibition of different genetic programs under control of various transcription factors (1, 26). Our gene expression analyses supported this view. In this study, we showed that the integrin signaling pathway is one of the pathways affecting myoblast fusion in CP. Integrins play a significant role in multiple aspects of skeletal muscle homeostasis, including maintenance of the SC niche, myoblast fusion, assembly of costameres and sarcomeres, development of the myotendinous and neuromuscular junctions, transduction of mechanical signals that lead to cytoskeletal rearrangements, and changes in gene expression (43, 44, 47, 54, 58, 61). Signaling through integrin-mediated FAK phosphorylation during myogenesis regulates the actin cytoskeleton, focal adhesions, Wnt, and MAPK signaling. It also causes overexpression of CAV3 and ITGB1D genes, which are some of the proteins involved in myoblast fusion whose gene expression was downregulated in CP myoblasts during differentiation (34, 42). Despite this strong evidence for a role of integrin signaling, it is fair to assume that impairment in other signaling pathways involved in myoblast fusion and myotube formation (e.g., TMEM8C/Myomaker, Rho GTPases, MAPKs, calcineurin- NFATc2, NF-κB, WNT, MMPs) may have significantly contributed to the decrease in myogenic potential of CP myoblasts (26, 37).

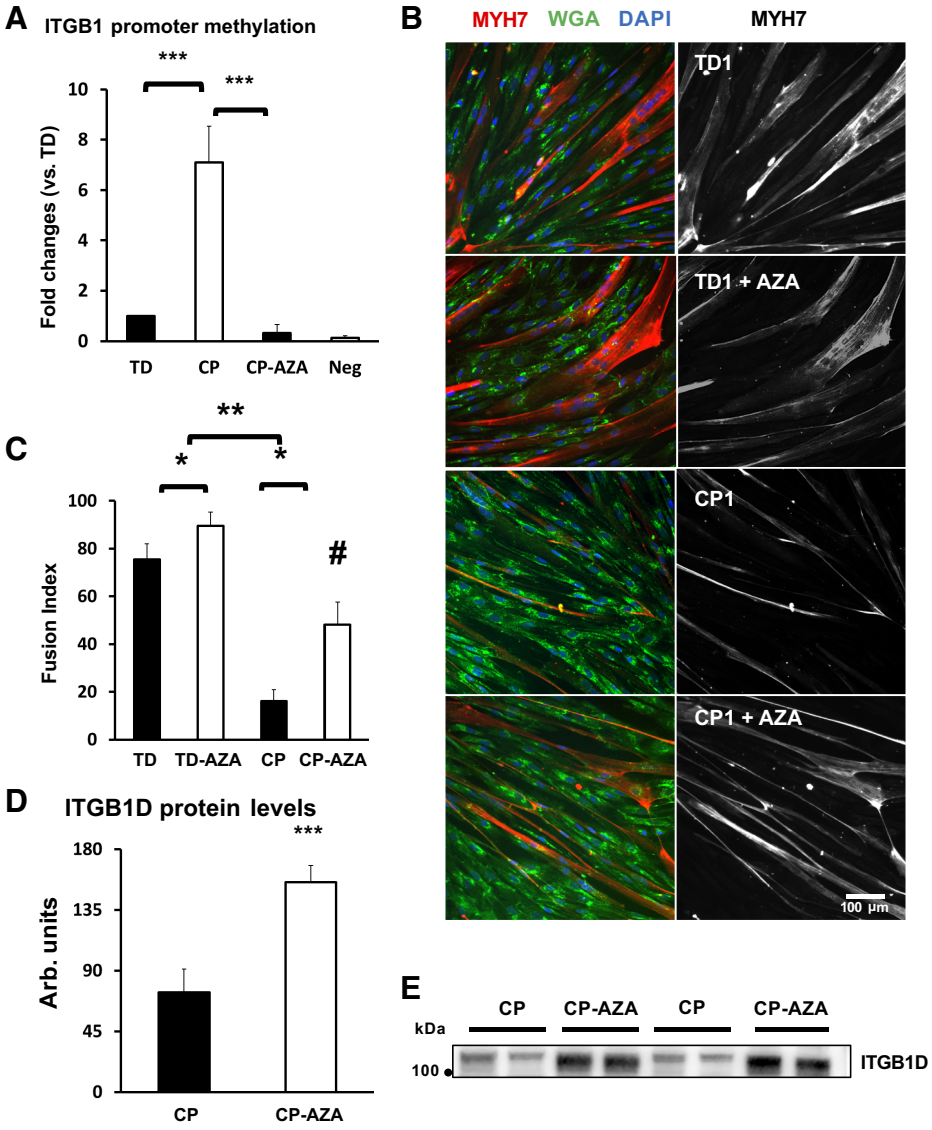

Fig. 6. 5-Azacytidine (5-AZA) rescues, integrin-β 1D (ITGB1D) expression and promotes myotube formation in cerebral palsy (CP). *A*: DNA methylation analysis of the CpG island located in the promoter region of the human ITGB1 gene in differentiating CP and typically developing (TD) myoblasts, pretreated (CP-AZA) or nonpretreated (CP, TD) with cytidine analog 5-AZA. Analysis was performed semi-quantitatively using "fold-change" estimates, where the nontreated TD group (TD) was set to the value of 1; ***TD vs. CP; ***CP vs. CP-AZA, $P < 0.001$; analysis by one-way ANOVA ($n = 4$/group). *B*: immunofluorescence staining for TD and CP myotube preparations, nontreated or pretreated with 5-AZA (+AZA). Myoblasts were differentiated for 42 h and then stained for myosin heavy chain 7 (MYH7; in red), and counterstained for membrane marker wheat germ agglutinin (WGA; in green) and nuclear marker DAPI (in blue). Gray scale panels show MYH7 staining as a separate channel. *C*: quantification of Fusion Index for CP and TD myoblasts nontreated or pretreated with 5-AZA (+AZA). Quantification was performed after 42 h of differentiation; *nontreated vs treated (+AZA), $P < 0.0001$; **CP vs TD, $P < 0.0001$; #CP treated with AZA, $P = 0.02$, analysis by two-way ANOVA ($N = 4$/group). *D*: protein quantification for ITGB1D by Western blotting in nontreated (CP) and pretreated (CP + AZA) myoblast cultures after 42 h differentiation; ***$P < 0.001$, analysis by one-way ANOVA ($n = 4$/group). *E*: representative Western blots showing differential expression of ITGB1D bands at ~116 kDa), in CP preparations nontreated (CP) or pretreated with 5-AZA (CP + AZA). Only significant *P* values are reported.

We also identified DNA methylation as a possible mechanism that adversely affects gene expression and impairs myoblast fusion in CP. This was confirmed by pretreatment of myoblast cultures with the demethylating agent 5-AZA, which improved differentiation in culture. Previous reports suggested that expression of specific key transcriptional regulators during myogenesis (MyoD, Myogenin, Myf5) were significantly affected by DNA methylation. Published studies using C2C12, human myoblasts, and/or embryonic stem cells showed that proliferating myoblasts treated with 5-AZA exhibited increased expression of muscle-specific genes, enhancing myotube maturation, whereas DNA hypomethylation in gene promoters was necessary for proliferating myoblasts to progress to the myotube stage (8, 27, 38, 56). For these reasons, we propose that hypermethylation of gene promoter regions associated with myoblast fusion in CP prevented these cells from proceeding through the myogenic program, resulting in impairment of muscle fiber formation.

On a broader scale, genome-wide DNA methylation studies showed that the majority of the DNA methylome remained relatively preserved during myogenic differentiation of adult satellite cells into myotubes (8, 56). Interestingly, a recent publication showed that the enzymatic procedures used to isolate and to sort satellite cells from adult tissue induced major transcriptional changes accompanied by histone modifications in these cells but did not involve significant alterations in DNA methylation patterns (33). These data suggest that DNA methylation is a very stable epigenetic "imprint" that is preserved in differentiated postmitotic tissue, as well as in tissue-committed adult stem cells (e.g., satellite cells). For these reasons, we speculate that the specific hypermethylation pattern that we observed on the promoter region of the ITGB1 gene in CP cell cultures represents a pathologic change of the early establishment of an epigenetic memory to keep cell fate commitment through the inheritance and maintenance of DNA methylation patterns during postnatal development. If confirmed, this would suggest that the impairment of myogenesis in contractured CP muscle could be the result of epigenetic and transcriptomic changes affecting development and commitment of early/embryonic muscle progenitors into Pax7-dependent adult

satellite cells, thus preceding the development of muscle contracture. An experimental analysis of DNA methylation and myogenic potential of these cells isolated at different developmental stages of CP using an experimental model (e.g., before and after brain injury in an animal model) could establish causality between epigenetic modifications and postnatal development of muscle contractures. One may also envision a clinical study where comparative methylation analyses could be performed on DNA extracted from serial blood samples obtained from developing children with CP. For therapeutic purposes, it is important to determine the genomic locations where DNA methylation affects myogenesis and myoblast fusion in CP and to establish whether demethylating agents like the cytidine analog 5-AZA could be used therapeutically to promote muscle development and treat muscle contractures in this patient population.

Future research will provide additional insight into the use of 5-AZA and its effects on muscle SC. For one, the clinical significance of a decreased myogenic potential of SCs in CP would be strengthened further by establishing a positive correlation between the extent of in vitro myoblast dysfunction with clinical parameters used to establish severity of contractures and gross motor function. This study relied on tissue samples from eight study subjects per group, and future studies with greater numbers of study subjects will further strengthen the relationship between in vitro biological observations and clinical parameters. Additionally, it would be important to investigate whether a decrease in myoblast homeostasis in cell culture is associated with a reduced capacity to regenerate functional muscle fibers after injury or surgical procedures using an in vivo model.

Overall, our findings suggest a new direction in the study of human muscle contractures by demonstrating the impact that impaired SC homeostasis plays on postnatal muscle growth and repair in children with CP. Under physiological conditions, skeletal muscle length increases as a result of the longitudinal growth of the component muscle fibers leads to a gain in muscle excursion and force generation (32). During the lengthening process, sarcomeres are added in series at the ends and sides of growing myofibrils by mechanisms of SC fusion and muscle fiber hypertrophy (2, 46, 59). In particular, the ends of skeletal muscle fibers and the myotendinous junction (the connection site between tendon and muscle fibers) are suggested to be rich in proliferating SCs and the preferential site for SC fusion and overall longitudinal muscle growth (3, 60). In children with CP, we suggest that the increase in muscle length and volume required to keep up with the changes in bone length during development is impaired, leading to musculoskeletal impairments that exacerbate with age. These impairments include shorter muscles and development of muscle contractures that significantly affect joint excursion and movement (4, 21, 35). Decreased capacity of the resident SC population to participate in new muscle fiber formation or repair following injury could directly impact postnatal development and promote contractures in CP. At the cellular level, muscle tissue complications in some children with CP are associated with a ~40% reduction in serial sarcomere number, i.e., the number of sarcomere units along the length of a fiber, leading to sarcomere lengthening and overstretching (36, 52). We previously demonstrated that these sarcomeric properties were associated with altered muscle transcriptional profiles, increased connective tissue, and a 60%–70% depletion of the resident SC number (14, 50, 53). Even though the relationship between sarcomere length, contractures, and SC homeostasis is still not fully understood, we speculate that in CP, fewer cells would successfully fuse with fibers and participate in muscle formation as children grow, leading to "stretched" muscle fibers with longer sarcomeres as previously reported (52). This possibility is supported by recent experimental work showing that stretch- and casting-induced sarcomere adaptation, muscle fiber lengthening, ankle range of motion, and connective tissue homeostasis were all impaired in mice with a preemptive 60%–70% deletion of their SC number (28). Furthermore, other studies established that impairment in SC function as a source of new myonuclei for nascent or regenerating fibers leads to diminution of the SC pool, changes in the tissue microenvironment, and increased tissue fibrosis, especially during aging or progression of muscle dystrophies (12, 13, 49).

The difference in age between groups is a confounding factor within this study as it was impossible to age match the two groups. However, importantly, the impaired myogenic potential of satellite cell-derived myoblasts in the younger population of children with CP may actually be an underestimate of the difference between groups, as younger children would be expected to have a greater satellite cell function and myogenic potential based solely on age. Thus, our results suggest a mechanism whereby the myogenic potential of satellite cell-derived myoblasts could limit muscle growth and repair in patients with CP.

GRANTS

This work was supported by NIH National Institute of Arthritis and Musculoskeletal and Skin Diseases Grants P30 AR-061303 and R01 AR-057393 and the Shirley Ryan AbilityLab.

DISCLOSURES

No conflicts of interest, financial or otherwise, are declared by the authors.

AUTHOR CONTRIBUTIONS

A.A.D. and R.L.L. conceived and designed research; A.A.D., M.A.M., R.P., L.A.S., and H.G.C. performed experiments; A.A.D., M.A.M., R.P., L.A.S., and L.Z. analyzed data; A.A.D., M.A.M., L.A.S., L.Z., H.G.C., and R.L.L. interpreted results of experiments; A.A.D. prepared figures; A.A.D. drafted manuscript; A.A.D., L.A.S., and R.L.L. edited and revised manuscript; A.A.D. and R.L.L. approved final version of manuscript.

REFERENCES

1. **Abmayr SM, Pavlath GK.** Myoblast fusion: lessons from flies and mice. *Development* 139: 641–656, 2012. doi:10.1242/dev.068353.
2. **Allen DL, Roy RR, Edgerton VR.** Myonuclear domains in muscle adaptation and disease. *Muscle Nerve* 22: 1350–1360, 1999. doi:10.1002/(SICI)1097-4598(199910)22:10<1350::AID-MUS3>3.0.CO;2-8.
3. **Allouh MZ, Yablonka-Reuveni Z, Rosser BW.** Pax7 reveals a greater frequency and concentration of satellite cells at the ends of growing skeletal muscle fibers. *J Histochem Cytochem* 56: 77–87, 2008. doi:10.1369/jhc.7A7301.2007.
4. **Barber L, Hastings-Ison T, Baker R, Barrett R, Lichtwark G.** Medial gastrocnemius muscle volume and fascicle length in children aged 2 to 5 years with cerebral palsy. *Dev Med Child Neurol* 53: 543–548, 2011. doi:10.1111/j.1469-8749.2011.03913.x.
5. **Barrett RS, Lichtwark GA.** Gross muscle morphology and structure in spastic cerebral palsy: a systematic review. *Dev Med Child Neurol* 52: 794–804, 2010. doi:10.1111/j.1469-8749.2010.03686.x.
6. **Boyle CA, Boulet S, Schieve LA, Cohen RA, Blumberg SJ, Yeargin-Allsopp M, Visser S, Kogan MD.** Trends in the prevalence of developmental disabilities in US children, 1997-2008. *Pediatrics* 127: 1034–1042, 2011. doi:10.1542/peds.2010-2989.

7. **Capkovic KL, Stevenson S, Johnson MC, Thelen JJ, Cornelison DD.** Neural cell adhesion molecule (NCAM) marks adult myogenic cells committed to differentiation. *Exp Cell Res* 314: 1553–1565, 2008. doi:10.1016/j.yexcr.2008.01.021.
8. **Carrió E, Díez-Villanueva A, Lois S, Mallona I, Cases I, Forn M, Peinado MA, Suelves M.** Deconstruction of DNA methylation patterns during myogenesis reveals specific epigenetic events in the establishment of the skeletal muscle lineage. *Stem Cells* 33: 2025–2036, 2015. doi:10.1002/stem.1998.
9. **Carrió E, Suelves M.** DNA methylation dynamics in muscle development and disease. *Front Aging Neurosci* 7: 19, 2015. doi:10.3389/fnagi.2015.00019.
10. **Chan G, Miller F.** Assessment and treatment of children with cerebral palsy. *Orthop Clin North Am* 45: 313–325, 2014. doi:10.1016/j.ocl.2014.03.003.
11. **Christensen D, Van Naarden Braun K, Doernberg NS, Maenner MJ, Arneson CL, Durkin MS, Benedict RE, Kirby RS, Wingate MS, Fitzgerald R, Yeargin-Allsopp M.** Prevalence of cerebral palsy, co-occurring autism spectrum disorders, and motor functioning - Autism and Developmental Disabilities Monitoring Network, USA, 2008. *Dev Med Child Neurol* 56: 59–65, 2014. doi:10.1111/dmcn.12268.
12. **Collins CA, Zammit PS, Ruiz AP, Morgan JE, Partridge TA.** A population of myogenic stem cells that survives skeletal muscle aging. *Stem Cells* 25: 885–894, 2007. doi:10.1634/stemcells.2006-0372.
13. **Conboy IM, Conboy MJ, Wagers AJ, Girma ER, Weissman IL, Rando TA.** Rejuvenation of aged progenitor cells by exposure to a young systemic environment. *Nature* 433: 760–764, 2005. doi:10.1038/nature03260.
14. **Dayanidhi S, Dykstra PB, Lyubasyuk V, McKay BR, Chambers HG, Lieber RL.** Reduced satellite cell number in situ in muscular contractures from children with cerebral palsy. *J Orthop Res* 33: 1039–1045, 2015. doi:10.1002/jor.22860.
15. **De Spiegelaere W, Dern-Wieloch J, Weigel R, Schumacher V, Schorle H, Nettersheim D, Bergmann M, Brehm R, Kliesch S, Vandekerckhove L, Fink C.** Reference gene validation for RT-qPCR, a note on different available software packages. *PLoS One* 10: e0122515, 2015. doi:10.1371/journal.pone.0122515.
16. **Dodd KJ, Taylor NF, Damiano DL.** A systematic review of the effectiveness of strength-training programs for people with cerebral palsy. *Arch Phys Med Rehabil* 83: 1157–1164, 2002. doi:10.1053/apmr.2002.34286.
17. **Dumont NA, Wang YX, Rudnicki MA.** Intrinsic and extrinsic mechanisms regulating satellite cell function. *Development* 142: 1572–1581, 2015. doi:10.1242/dev.114223.
18. **Farmer SR.** Regulation of PPARgamma activity during adipogenesis. *Int J Obes* 29, *Suppl* 1: S13–S16, 2005. doi:10.1038/sj.ijo.0802907.
19. **Fong AP, Yao Z, Zhong JW, Cao Y, Ruzzo WL, Gentleman RC, Tapscott SJ.** Genetic and epigenetic determinants of neurogenesis and myogenesis. *Dev Cell* 22: 721–735, 2012. doi:10.1016/j.devcel.2012.01.015.
20. **Gillett JG, Boyd RN, Carty CP, Barber LA.** The impact of strength training on skeletal muscle morphology and architecture in children and adolescents with spastic cerebral palsy: A systematic review. *Res Dev Disabil* 56: 183–196, 2016. doi:10.1016/j.ridd.2016.06.003.
21. **Gough M, Shortland AP.** Could muscle deformity in children with spastic cerebral palsy be related to an impairment of muscle growth and altered adaptation? *Dev Med Child Neurol* 54: 495–499, 2012. doi:10.1111/j.1469-8749.2012.04229.x.
22. **Graham HK, Rosenbaum P, Paneth N, Dan B, Lin JP, Damiano DL, Becher JG, Gaebler-Spira D, Colver A, Reddihough DS, Crompton KE, Lieber RL.** Cerebral palsy. *Nat Rev Dis Primers* 2: 15082, 2016. doi:10.1038/nrdp.2015.82.
23. **Gray L, Ng H, Bartlett D.** The gross motor function classification system: an update on impact and clinical utility. *Pediatr Phys Ther* 22: 315–320, 2010. doi:10.1097/PEP.0b013e3181ea8e52.
24. **Hägglund G, Andersson S, Düppe H, Lauge-Pedersen H, Nordmark E, Westbom L.** Prevention of severe contractures might replace multilevel surgery in cerebral palsy: results of a population-based health care programme and new techniques to reduce spasticity. *J Pediatr Orthop B* 14: 269–273, 2005 [Erratum in *J Pediatr Orthop B* 14: 388, 2005]. doi:10.1097/01202412-200507000-00007.
25. **Hildyard JC, Wells DJ.** Identification and validation of quantitative PCR reference genes suitable for normalizing expression in normal and dystrophic cell culture models of myogenesis. *PLoS Curr* 6: ecurrents.md.faafdde4bea8df4aa7d06cd5553119a6, 2014. doi:10.1371/currents.md.faafdde4bea8df4aa7d06cd5553119a6.
26. **Hindi SM, Tajrishi MM, Kumar A.** Signaling mechanisms in mammalian myoblast fusion. *Sci Signal* 6: re2, 2013. doi:10.1126/scisignal.2003832.
27. **Hupkes M, Jonsson MK, Scheenen WJ, van Rotterdam W, Sotoca AM, van Someren EP, van der Heyden MA, van Veen TA, van Ravestein-van Os RI, Bauerschmidt S, Piek E, Ypey DL, van Zoelen EJ, Dechering KJ.** Epigenetics: DNA demethylation promotes skeletal myotube maturation. *FASEB J* 25: 3861–3872, 2011. doi:10.1096/fj.11-186122.
28. **Kinney MC, Dayanidhi S, Dykstra PB, McCarthy JJ, Peterson CA, Lieber RL.** Reduced skeletal muscle satellite cell number alters muscle morphology after chronic stretch but allows limited serial sarcomere addition. *Muscle Nerve* 55: 384–392, 2017. doi:10.1002/mus.25227.
29. **Laker RC, Ryall JG.** DNA methylation in skeletal muscle stem cell specification, proliferation, and differentiation. *Stem Cells Int* 2016: 5725927, 2016. doi:10.1155/2016/5725927.
30. **Laumonier T, Menetrey J.** Muscle injuries and strategies for improving their repair. *J Exp Orthop* 3: 15, 2016. doi:10.1186/s40634-016-0051-7.
31. **Lepper C, Partridge TA, Fan CM.** An absolute requirement for Pax7-positive satellite cells in acute injury-induced skeletal muscle regeneration. *Development* 138: 3639–3646, 2011. doi:10.1242/dev.067595.
32. **Lieber RL, Ward SR.** Skeletal muscle design to meet functional demands. *Philos Trans R Soc Lond B Biol Sci* 366: 1466–1476, 2011. doi:10.1098/rstb.2010.0316.
33. **Machado L, Esteves de Lima J, Fabre O, Proux C, Legendre R, Szegedi A, Varet H, Ingerslev LR, Barrès R, Relaix F, Mourikis P.** In situ fixation redefines quiescence and early activation of skeletal muscle stem cells. *Cell Rep* 21: 1982–1993, 2017. doi:10.1016/j.celrep.2017.10.080.
34. **Madaro L, Marrocco V, Fiore P, Aulino P, Smeriglio P, Adamo S, Molinaro M, Bouché M.** PKCθ signaling is required for myoblast fusion by regulating the expression of caveolin-3 and β1D integrin upstream focal adhesion kinase. *Mol Biol Cell* 22: 1409–1419, 2011. doi:10.1091/mbc.e10-10-0821.
35. **Mathewson MA, Lieber RL.** Pathophysiology of muscle contractures in cerebral palsy. *Phys Med Rehabil Clin N Am* 26: 57–67, 2015. doi:10.1016/j.pmr.2014.09.005.
36. **Mathewson MA, Ward SR, Chambers HG, Lieber RL.** High resolution muscle measurements provide insights into equinus contractures in patients with cerebral palsy. *J Orthop Res* 33: 33–39, 2015. doi:10.1002/jor.22728.
37. **Millay DP, O'Rourke JR, Sutherland LB, Bezprozvannaya S, Shelton JM, Bassel-Duby R, Olson EN.** Myomaker is a membrane activator of myoblast fusion and muscle formation. *Nature* 499: 301–305, 2013. doi:10.1038/nature12343.
38. **Montesano A, Luzi L, Senesi P, Terruzzi I.** Modulation of cell cycle progression by 5-azacytidine is associated with early myogenesis induction in murine myoblasts. *Int J Biol Sci* 9: 391–402, 2013. doi:10.7150/ijbs.4729.
39. **Murphy SM, Kiely M, Jakeman PM, Kiely PA, Carson BP.** Optimization of an in vitro bioassay to monitor growth and formation of myotubes in real time. *Biosci Rep* 36: e00330, 2016. doi:10.1042/BSR20160036.
40. **Novak I, Hines M, Goldsmith S, Barclay R.** Clinical prognostic messages from a systematic review on cerebral palsy. *Pediatrics* 130: e1285–e1312, 2012. doi:10.1542/peds.2012-0924.
41. **Pavone V, Testa G, Restivo DA, Cannavò L, Condorelli G, Portinaro NM, Sessa G.** Botulinum toxin treatment for limb spasticity in childhood cerebral palsy. *Front Pharmacol* 7: 29, 2016. doi:10.3389/fphar.2016.00029.
42. **Quach NL, Biressi S, Reichardt LF, Keller C, Rando TA.** Focal adhesion kinase signaling regulates the expression of caveolin 3 and beta1 integrin, genes essential for normal myoblast fusion. *Mol Biol Cell* 20: 3422–3435, 2009. doi:10.1091/mbc.e09-02-0175.
43. **Quach NL, Rando TA.** Focal adhesion kinase is essential for costamerogenesis in cultured skeletal muscle cells. *Dev Biol* 293: 38–52, 2006. doi:10.1016/j.ydbio.2005.12.040.
44. **Rozo M, Li L, Fan CM.** Targeting β1-integrin signaling enhances regeneration in aged and dystrophic muscle in mice. *Nat Med* 22: 889–896, 2016. doi:10.1038/nm.4116.
45. **Sambasivan R, Yao R, Kissenpfennig A, Van Wittenberghe L, Paldi A, Gayraud-Morel B, Guenou H, Malissen B, Tajbakhsh S, Galy A.** Pax7-expressing satellite cells are indispensable for adult skeletal muscle

regeneration. *Development* 138: 3647–3656, 2011. doi:10.1242/dev.067587.

46. **Sanger JW, Chowrashi P, Shaner NC, Spalthoff S, Wang J, Freeman NL, Sanger JM.** Myofibrillogenesis in skeletal muscle cells. *Clin Orthop Relat Res* 403, *Suppl*: S153–S162, 2002. doi:10.1097/00003086-200210001-00018.
47. **Schwander M, Shirasaki R, Pfaff SL, Müller U.** Beta1 integrins in muscle, but not in motor neurons, are required for skeletal muscle innervation. *J Neurosci* 24: 8181–8191, 2004. doi:10.1523/JNEUROSCI.1345-04.2004.
48. **Sente T, Van Berendoncks AM, Fransen E, Vrints CJ, Hoymans VY.** Tumor necrosis factor-α impairs adiponectin signalling, mitochondrial biogenesis, and myogenesis in primary human myotubes cultures. *Am J Physiol Heart Circ Physiol* 310: H1164–H1175, 2016. doi:10.1152/ajpheart.00831.2015.
49. **Shefer G, Van de Mark DP, Richardson JB, Yablonka-Reuveni Z.** Satellite-cell pool size does matter: defining the myogenic potency of aging skeletal muscle. *Dev Biol* 294: 50–66, 2006. doi:10.1016/j.ydbio.2006.02.022.
50. **Smith LR, Chambers HG, Lieber RL.** Reduced satellite cell population may lead to contractures in children with cerebral palsy. *Dev Med Child Neurol* 55: 264–270, 2013. doi:10.1111/dmcn.12027.
51. **Smith LR, Chambers HG, Subramaniam S, Lieber RL.** Transcriptional abnormalities of hamstring muscle contractures in children with cerebral palsy. *PLoS One* 7: e40686, 2012. doi:10.1371/journal.pone.0040686.
52. **Smith LR, Lee KS, Ward SR, Chambers HG, Lieber RL.** Hamstring contractures in children with spastic cerebral palsy result from a stiffer extracellular matrix and increased in vivo sarcomere length. *J Physiol* 589: 2625–2639, 2011. doi:10.1113/jphysiol.2010.203364.
53. **Smith LR, Pontén E, Hedström Y, Ward SR, Chambers HG, Subramaniam S, Lieber RL.** Novel transcriptional profile in wrist muscles from cerebral palsy patients. *BMC Med Genomics* 2: 44, 2009. doi:10.1186/1755-8794-2-44.
54. **Sparrow JC, Schöck F.** The initial steps of myofibril assembly: integrins pave the way. *Nat Rev Mol Cell Biol* 10: 293–298, 2009. doi:10.1038/nrm2634.
55. **Taylor SM.** 5-Aza-2′-deoxycytidine: cell differentiation and DNA methylation. *Leukemia* 7, *Suppl* 1: 3–8, 1993.
56. **Tsumagari K, Baribault C, Terragni J, Varley KE, Gertz J, Pradhan S, Badoo M, Crain CM, Song L, Crawford GE, Myers RM, Lacey M, Ehrlich M.** Early de novo DNA methylation and prolonged demethylation in the muscle lineage. *Epigenetics* 8: 317–332, 2013. doi:10.4161/epi.23989.
57. **Van Naarden Braun K, Doernberg N, Schieve L, Christensen D, Goodman A, Yeargin-Allsopp M.** Birth prevalence of cerebral palsy: a population-based study. *Pediatrics* 137: e20152872, 2016. doi:10.1542/peds.2015-2872.
58. **Wang HV, Chang LW, Brixius K, Wickström SA, Montanez E, Thievessen I, Schwander M, Müller U, Bloch W, Mayer U, Fässler R.** Integrin-linked kinase stabilizes myotendinous junctions and protects muscle from stress-induced damage. *J Cell Biol* 180: 1037–1049, 2008. doi:10.1083/jcb.200707175.
59. **Williams PE, Goldspink G.** Longitudinal growth of striated muscle fibres. *J Cell Sci* 9: 751–767, 1971.
60. **Zhang M, McLennan IS.** During secondary myotube formation, primary myotubes preferentially absorb new nuclei at their ends. *Dev Dyn* 204: 168–177, 1995. doi:10.1002/aja.1002040207.
61. **Zhang SJ, Truskey GA, Kraus WE.** Effect of cyclic stretch on β1D-integrin expression and activation of FAK and RhoA. *Am J Physiol Cell Physiol* 292: C2057–C2069, 2007. doi:10.1152/ajpcell.00493.2006.